THE JOURNAL OF PHYSICAL CHEMISTRY Letters

LETTER

pubs.acs.org/JPCL

Surface-Enhanced Raman Spectroelectrochemistry of TTF-Modified Self-Assembled Monolayers

Walter F. Paxton,[†] Samuel L. Kleinman, Ashish N. Basuray, J. Fraser Stoddart,* and Richard P. Van Duyne*

Department of Chemistry, Northwestern University, 2145 Sheridan Road, Evanston, Illinois 60208-3113, United States

Supporting Information

ABSTRACT: Surface-enhanced Raman spectroscopy (SERS) was used to monitor the response of a self-assembled monolayer (SAM) of a tetrathiafulvalene (TTF) derivative on a gold film-over-nanosphere electrode. The electrochemical response observed was rationalized in terms of the interactions between TTF moieties as the oxidation state was changed. Electrochemical oxidation to form the monocation caused the absorbance of the TTF unit to coincide with both the laser excitation wavelength and the localized surface plasmon resonance (LSPR), resulting in surface-enhanced resonance Raman scattering (SERRS). The vibrational frequency changes that accompany electron transfer afford a high-contrast mechanism that can be used to determine the oxidation state of the TTF unit in an unambiguous manner.

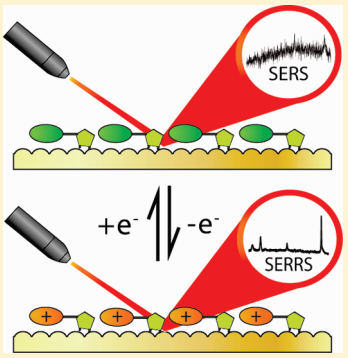

SECTION: Kinetics, Spectroscopy

Tetrathiafulvalene (TTF) is an electron-rich redox-active molecule that has been utilized extensively in mechano-stereochemical systems[1] and molecular electronic devices[2−5] (MEDs). Neutral TTF is capable of donating one or two electrons to yield stable singly and doubly charged states, permitting access to electrochemically addressable electronic and magnetic properties.[6] It also has the benefit of preserving its electrochemical properties following substitution at any or all four of its exterior carbons, thus enriching its chemical diversity by extending its utility to functionalized TTF molecules.[7] For these reasons, TTF has been investigated extensively as an electroactive recognition element in bistable mechanically interlocked molecules (MIMs) in solution,[8] in polymer matrices,[9] in self-assembled monolayers (SAMs) on gold electrodes[10] and on gold nanoparticles,[11] in closely packed condensed monolayers,[12,13] in Langmuir−Blodgett films mounted on solid supports, and in molecular switch tunnel junctions[14] (MSTJs). Over the past decade,[15−19] numerous reports, supported by molecular dynamics simulations,[20,21] have documented the integration of bistable MIMs (where TTF is one of the key electroactive recognition elements) into MSTJs in solid-state MEDs. Although the incorporation of the bistable MIMs containing TTF as the switching trigger in the integrated systems and devices is a highly promising development offering considerable potential for the future growth of MEDs, direct real-time evidence for physical motion in response to electrochemical stimulation in these devices remains sparse.

Vibrational spectroscopy, such as Raman scattering, has the ability to resolve the identity of a molecule and report changes in its chemical structure and oxidation state, providing direct spectroscopic evidence of structural changes in real time. Surface-enhanced Raman spectroscopy (SERS) can amplify the vibrational signal on substrates that exhibit a localized surface plasmon resonance (LSPR). The technique is most effective when the LSPR peak frequency is well-matched[22] to the laser excitation wavelength (λ_{ex}). SERS may be further enhanced by the resonance Raman effect if an electronic transition of the molecule of interest overlaps with λ_{ex}, known as surface-enhanced resonance Raman spectroscopy (SERRS). SERRS has recently been observed in a supramolecular system to monitor the association of a TTF and cyclobis(paraquat-*p*-phenylene) in solution.[23] Since its inception, SERS has been used to investigate submonolayer coverages of molecules, providing information regarding charge state, physical orientation, and local environment. Resonance Raman spectroscopy,[24−28] SERS,[29] as well as SERRS[30,31] have been widely used to investigate TTF and its derivatives both in the solid state and in solution, revealing large vibrational frequency changes corresponding to different oxidation states.

The electrochemistry of TTF in nonaqueous solution is well characterized. TTF exhibits two reversible one-electron processes at approximately 0.34 and 0.68 V (vs SCE), as observed via cyclic voltammetry (CV) and other electrochemical methods.[25] Appropriately functionalized TTF derivatives have allowed the investigation of the electrochemical properties of SAMs of TTF adsorbed onto electrodes, for example, TTF with pendent thiol or dithiolane groups adsorbed to gold, yielding important insight into the effect of intermolecular interactions between neighboring TTF units.[7,32−34]

Here, we carry out SER spectroelectrochemistry to investigate the redox properties and structural changes of **1** (Figure 1)

Received: April 18, 2011
Accepted: April 19, 2011

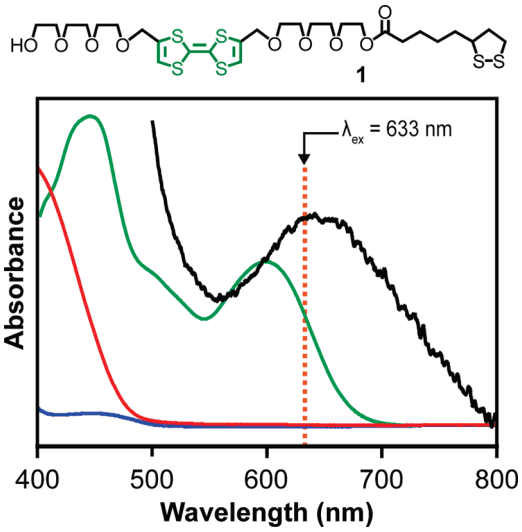

Figure 1. Structural formula of the TTF derivative **1** (top) and the truncated UV−vis absorbance spectra of 0.1 mM **1** in MeCN in its neutral (**1**, blue trace), radical cationic ($\mathbf{1}^{\bullet+}$, green trace), and dicationic ($\mathbf{1}^{2+}$, red trace) forms. Also shown is the wavelength (λ_{ex}) of the excitation source and the normalized absorbance spectrum of the SERS-active AuFON electrode (black trace), revealing the LSPR band centered at 640 nm. Taken together, this figure illustrates the matching between the $\mathbf{1}^{\bullet+}$ absorbance, the AuFON LSPR, and λ_{ex}. See Supporting Information for the complete UV−vis data for **1** in various oxidation states, as well as the oxidation procedure.

bound to the surface of a SERS-active working electrode. To this end, we prepared gold film-over-nanosphere (AuFON) electrode surfaces using nanosphere lithography[35] (see Supporting Information for fabrication details). Gold is attractive, not only for its plasmonic properties[36] but also because of its utility as an electrode material[37] and as a substrate for the formation of SAMs.[38] Figure 1 shows the absorbance spectrum (−log(reflectance)) of the AuFON, indicating that the peak of the LSPR is straddling the 633 nm excitation source and Stokes-shifted wavelengths, an ideal situation for SERS.[22] In addition to the spectral overlap of the laser excitation wavelength and the LSPR maximum of the AuFON, Figure 1 shows the visible absorption spectra of **1** for all three oxidation states. Both the neutral and doubly oxidized states of **1** are not in resonance with λ_{ex}. In contrast, the radical cation $\mathbf{1}^{\bullet+}$ exhibits an electronic transition that coincides with both the LSPR of the AuFON and λ_{ex}. In this case, SERRS provides signal enhancement by greater than a factor of 30 over SERS, demonstrated in the following spectra. By controlling the electrochemical potential of the TTF moieties, we introduce an externally controlled contrast mechanism for turning on and off the resonance enhancement in SER(R)S.

Following fabrication, AuFON electrodes were incubated overnight in 1 mM **1** in MeCN to promote SAM formation. Electrodes were rinsed liberally with fresh MeCN prior to spectroelectrochemical analysis. AuFON working electrodes were mounted in a custom-built Teflon-body spectroelectrochemical cell with a silver wire (Ag/Ag^+) quasi-reference electrode and a platinum counter electrode; the electrolyte solution was 0.1 M $LiClO_4$ in MeCN. The electrochemistry of the resulting AuFON electrodes modified with a SAM of **1** was probed by CV. Figure 2 shows a cyclic voltammogram of the AuFON electrode coated with a SAM of **1** obtained at 10 mV/s. Two reversible one-electron transfer processes separated by 400 mV are observed.

The separation between the potentials (ΔE_p) for the oxidation and the reduction peaks for each redox process was approximately 10 mV, consistent with a surface-bound electroactive species. Further evidence of surface-bound activity was obtained through variable scan rate CV, revealing that both anodic and cathodic peak currents for each one-electron process scaled linearly with scan rate[37] (Figure S5, Supporting Information). The electrode area was measured electrochemically for identically prepared AuFON electrodes from the hydrogen desorption peak in 1 M H_2SO_4. The total charge passed for each reduction and the oxidation peak was between 1.01 and 1.11 μC, indicating that nearly all electroactive species underwent complete changes in oxidation state during the potential scan. This information was combined with surface area measurements to determine the surface excess of **1** to be $\Gamma = 9.1 \times 10^{-11}$ mol/cm^2, assuming $n = 1$. Previous literature precedent has suggested a surface excess of $3.1 \pm 0.5 \times 10^{-10}$ mol/cm^2 for a SAM composed of purely thioctic acid on Au.[39] The surface excess of **1** is more than three times lower than that for a "more ideal" SAM system.[40,41] We justify this observation in two ways. One, the TTF derivative **1** is relatively larger than thioctic acid, implying that less **1** would fit per unit area on a surface. Two, if the TTF moiety in **1** were lying down on the surface (as opposed to standing up normal to the surface), then molecules of **1** would pack less efficiently, accounting for the reduced coverage. We employed computational modeling[42] to assess the size of **1** and give insight into the orientation on the surface. Assuming that the long axis of **1** is parallel to the surface, we find a maximum surface excess of 9.1×10^{-11} mol/cm^2, in agreement with experimentally measured values. The parallel orientation would cause most vibrations of **1** to be forbidden as a result of surface selection rules.[43] This effect is manifested in the weak SERS spectra, implying that SERRS is necessary to obtain data with good signal-to-noise ratios, exemplified by our spectra.

Previous explorations of the electrochemistry of TTF derivative SAMs demonstrated that the full width at half-maximum (fwhm) of both one-electron peaks deviates substantially from the ideal fwhm of 90 mV. We observed oxidation and reduction peaks of the first and second redox processes with fwhms of ∼160 and 60 mV, respectively. The presence of electrochemical

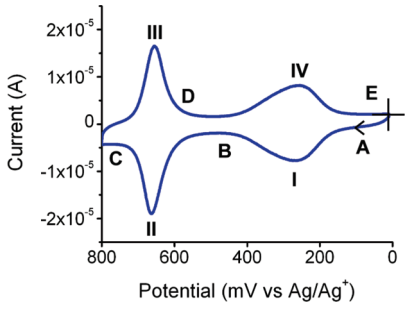

Figure 2. CV of a AuFON electrode coated in a SAM of **1** in 0.1 M $LiClO_4$ in MeCN with Ag/Ag^+ reference and Pt counter electrodes. Two reversible one-electron redox processes for the TTF unit are observed. The CV scan rate was 10 mV/s to allow simultaneous acquisition of SER(R) spectra at different electrode potentials. Labels A−E correspond to the spectra in Figure 4 collected at 50, 450, 750, 640, and 40 mV in turn. A and E correspond to **1**, B and D to $\mathbf{1}^{\bullet+}$, and C to $\mathbf{1}^{2+}$.

peaks that are both narrower and wider than the ideal 90 mV fwhm suggests that the observed effect is a result of the adsorbate SAM and not an artifact of surface-driven kinetics. This deviation is presumably caused by the interaction of neighboring redox centers. Intermolecular interactions can be prevented by diluting the surface concentration of **1** with a non-redox-active compound such as thioctic acid.[7] Hence, we created mixed monolayers of thioctic acid and **1** on Au substrates and found that the redox peaks arising from diluted **1** in the mixed monolayers of thioctic acid approached the ideal fwhm of 90 mV as the surface concentration of **1** dropped to <20% (Figure S6, Supporting Information). Assuming homogeneous dilution, this finding suggests an interaction of TTF moieties in close proximity, which causes deviations from ideality. Previous authors[34,44−46] have assigned attractive interactions for the $TTF/TTF^{\bullet+}$ redox couple, causing a distribution of energies that are required for the electrochemical transformation and therefore a larger fwhm. The $TTF^{\bullet+}/TTF^{2+}$ redox couple displays a fwhm that is substantially more narrow than ideal, which we assign to repulsive interactions between $TTF^{\bullet+}$ and TTF^{2+}.

To understand the interaction in more detail, the SERS response of **1** in different oxidation states was measured. SER spectra were acquired at 0, +500, and +800 mV, corresponding to neutral **1**, the radical cation $\mathbf{1}^{\bullet+}$, and the dicationic $\mathbf{1}^{2+}$, respectively (Figure 3). Consistent with earlier reports, the SER spectrum of the neutral **1** collected at 0 mV was not easy to resolve.[30] Only one vibrational mode at ∼490 cm^{-1} was

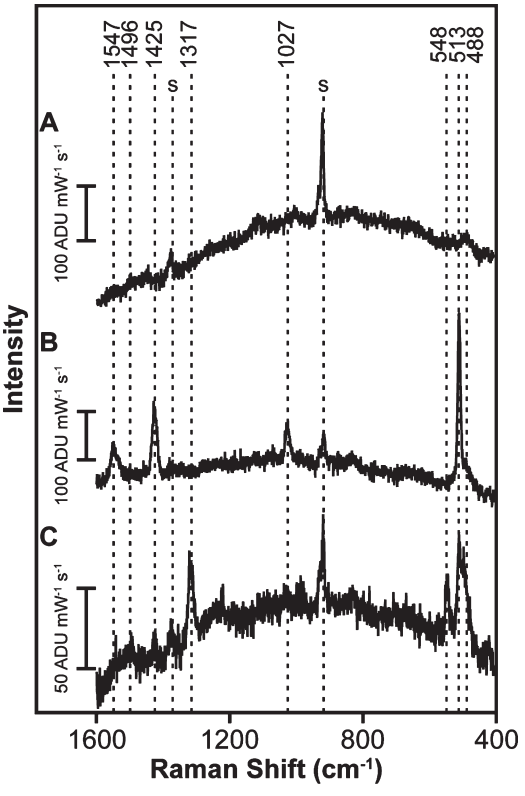

Figure 3. Potentiostatic surface-enhanced Raman spectra of a **1** monolayer in its various oxidation states on a AuFON electrode held at 0 (A), 500 (B), and 800 (C) mV. The corresponding spectral acquisition times were 100, 40, and 100 s with a laser power of 61 μW. λ_{ex} = 633 nm. Signals resulting from the MeCN are labeled s. Vertical scale bars are in units of ADU mW^{-1} s^{-1} (analog to digital units per milliwatt-second).

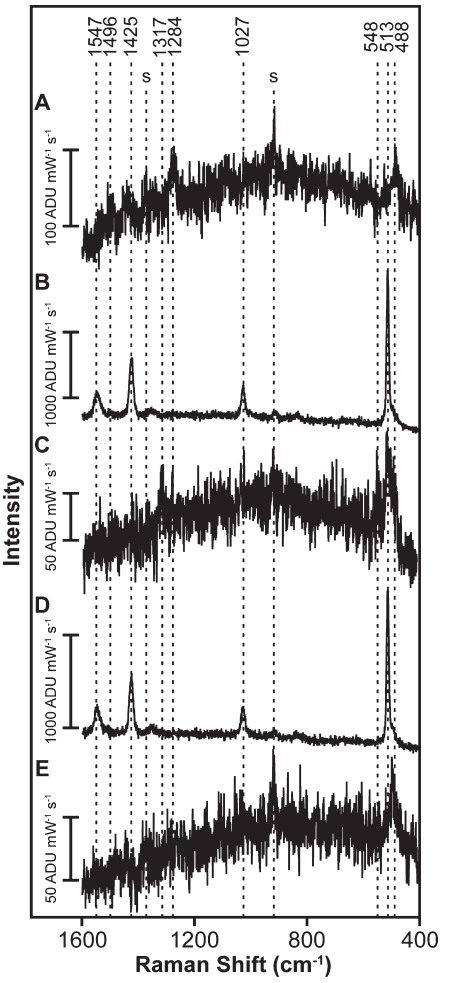

Figure 4. Potentiodynamic SER spectra of a monolayer of **1** in various oxidation states along the cyclic voltammogram shown in Figure 2. A−E correspond to electrode potentials of 50, 450, 750, 640, and 40 mV, in turn (vs Ag/Ag^{+}). Note the intensity scales for each spectrum. The dramatic change in signal as the potential is raised from 50 to 450 mV is the result of resonance enhancement as the neutral TTF (A) is oxidized to the radical cation $\mathbf{1}^{\bullet+}$ (B), a species which absorbs at λ_{ex} = 633 nm. Further oxidation to the dication $\mathbf{1}^{2+}$ (C) turns the resonance enhancement off. This process is reversible because the same behavior is observed on the return scan with the reduction of $\mathbf{1}^{2+}$ to the resonant $\mathbf{1}^{\bullet+}$ (D) and finally to neutral **1** (E). Acquisitions were 10 s using an excitation power of 61 μW. λ_{ex} = 633 nm. Signals resulting from the MeCN are labeled s. Vertical scale bars are in units of ADU mW^{-1} s^{-1} (analog to digital units per milliwatt−second).

observed above the noise and was assigned[25,29] to the stretching of the C−S bonds of the TTF unit. The increased signal intensity in Figure 3B is due to SERRS as the electrochemical potential was changed to +500 mV. Consistent with previous observations, the C−S stretching mode frequency shifts to 513 cm^{-1} as a result of the change in oxidation state.[25,26,29] Furthermore, the SERR signal allowed the observation of three additional bands at 1027, 1426, and 1547 cm^{-1}. The band at 1027 cm^{-1} is assigned to the first overtone of the C−S stretching mode at 513 cm^{-1}.[27] The resonance-induced appearance of a C−C stretching modes of the individual heterocycles accounts for the peaks at 1426 and 1547 cm^{-1}.[26] Interestingly, the peak at 1547 cm^{-1} has a shoulder at 1539 cm^{-1}, which is the second overtone of the C−S

dx.doi.org/10.1021/jz200523q | J. Phys. Chem. Lett. 2011, 2, 1145–1149

stretching mode. The spectrum of $\mathbf{1}^{2+}$ acquired at +800 mV exhibited signal intensity significantly attenuated relative to that in the $\mathbf{1}^{\bullet+}$ spectrum, with concomitant peak shifts of two major bands to 548 and 1317 cm^{-1}. The observed 109 cm^{-1} shift of the C−C stretch from 1426 to 1317 cm^{-1} as **1** was oxidized from the radical cation to the dication is in remarkably good agreement with a previous report of a 110 cm^{-1} shift between monocationic and dicationic TTF derivatives using resonance Raman spectroscopy.[25,26]

We observed marked spectroscopic differences between the different oxidation states of the SAM of **1** on a AuFON electrode under potentiostatic conditions. It is also possible to observe the changes in **1** under potentiodynamic conditions over the course of a cyclic potential scan. We collected a series of spectra concomitant with CV measurements of the monolayer of **1** on the AuFON surface. Each 10 s acquisition provided a real-time snapshot of the oxidation state of **1** as a function of the electrode potential over the course of the scan. The spectrum (Figure 4A) of neutral **1** revealed a peak at 488 cm^{-1} previously observed in the potentiostatic SERS measurements. Figure 4B shows the appearance of the vibrational modes at 513, 1027, 1425, and 1547 cm^{-1} as the potential of the AuFON increased beyond 270 mV. The overlap of a $\mathbf{1}^{\bullet+}$ electronic transition at 600 nm and the 633 nm excitation source causes SERRS, allowing the observation of many more vibrations. Figure 4C illustrates the lack of resonance enhancement for the dicationic $\mathbf{1}^{2+}$. The subsequent reduction portion of the voltammogram highlights the control and reversibility of both the electrochemistry and the SER(R)S of the monolayer.

We have demonstrated that a synergy of both surface and resonance Raman enhancement can be exploited to elucidate chemical information in real time about the oxidation state of molecules at an electrode interface. Electrochemical investigations indicate that nonidealities in the electrochemistry can be suppressed by diluting the surface concentration of redox-active compounds with an inert compound, suggesting that they arise as a result of the interactions between neighboring TTF units. The SER(R)S investigations revealed changes in vibrational frequencies of the TTF unit as a result of changes in oxidation state. Upon oxidation to the radical cation, the spectrum of **1** is greatly enhanced by resonance between λ_{ex} and the electronic absorbance of **1**. This highly sensitive contrast mechanism can be used to probe the state of TTF-bearing components in functional MEDs. The enhancement is sufficient to allow the observation of the first and second overtones of the C−S stretching mode. This nondestructive approach may allow the chemical interrogations of molecular switching events at interfaces in working MEDs in situ to enable the elucidation of processes involved in the response of switchable molecules to electronic stimulation.

■ ASSOCIATED CONTENT

Ⓢ Supporting Information. Synthesis and characterization of **1**, UV−vis spectroscopy, spectroelectrochemical details, and supporting electrochemistry. This material is available free of charge via the Internet at http://pubs.acs.org.

■ AUTHOR INFORMATION

Corresponding Author

*E-mail: stoddart@northwestern.edu (J.F.S.); vanduyne@northwestern.edu (R.P.V.D).

Present Addresses

[†]Center for Integrated Nanotechnologies (CINT), Sandia National Laboratories, Albuquerque, New Mexico, 87185.

■ ACKNOWLEDGMENT

This research was sponsored by the National Science Foundation (CHE-0911145, DMR0520513), and by the Air Force Office of Scientific Research under AFOSR/DARPA Project BAA07-61 (FA9550-08-1-0221) and AFOSR/MURI (FA9550-07-1-0534).

■ REFERENCES

(1) Olson, M. A.; Botros, Y. Y.; Stoddart, J. F. Mechanostereochemistry. *Pure Appl. Chem.* **2010**, *82*, 1569–1574.

(2) Flood, A. H.; Stoddart, J. F.; Steuerman, D. W.; Heath, J. R. Whence Molecular Electronics? *Science* **2004**, *306*, 2055–2056.

(3) Dichtel, W. R.; Heath, J. R.; Stoddart, J. F. Designing Bistable [2]Rotaxanes for Molecular Electronic Devices. *Philos. Trans. R. Soc. London, Ser. A* **2007**, *365*, 1607–1625.

(4) Heath, J. R. Molecular Electronics. *Annu. Rev. Mater. Sci.* **2009**, *39*, 1–23.

(5) van der Molen, S. J.; Liljeroth, P. Charge Transport Through Molecular Switches. *J. Phys.: Condens. Matter* **2010**, *22*, 1–30.

(6) Kuo, K.-N.; Moses, P. R.; Lenhard, J. R.; Green, D. C.; Murray, R. W. Immobilization, Electrochemistry, and Surface Interactions of Tetrathiafulvalene on Chemically Modified Ruthenium and Platinum Oxide Electrodes. *Anal. Chem.* **1979**, *51*, 745–748.

(7) Blanchard, P.-Y.; Alévêque, O.; Boisard, S.; Gautier, C.; El-Ghayoury, A.; Le Derf, F.; Breton, T.; Levillain, E. Intermolecular Interactions in Self-Assembled Monolayers of Tetrathiafulvalene Derivatives. *Phys. Chem. Chem. Phys.* **2011**, *13*, 2118–2120.

(8) Flood, A. H.; Peters, A. J.; Vignon, S. A.; Steuerman, D. W.; Tseng, H.-R.; Kang, S.; Heath, J. R.; Stoddart, J. F. The Role of Physical Environment on Molecular Electromechanical Switching. *Chem.—Eur. J.* **2004**, *10*, 6558–6564.

(9) Choi, J. W.; Flood, A. H.; Steuerman, D. W.; Nygaard, S.; Braunschweig, A. B.; Moonen, N. N. P.; Laursen, B. W.; Luo, Y.; DeIonno, E.; Peters, A. J. Ground-State Equilibrium Thermodynamics and Switching Kinetics of Bistable [2]Rotaxanes Switched in Solution, Polymer Gels, and Molecular Electronic Devices. *Chem.—Eur. J.* **2006**, *12*, 261–279.

(10) Tseng, H.-R.; Wu, D.; Fang, N. X.; Zhang, X.; Stoddart, J. F. The Metastability of an Electrochemically Controlled Nanoscale Machine on Gold Surfaces. *ChemPhysChem* **2004**, *5*, 111–116.

(11) Coskun, A.; Wesson, P. J.; Klajn, R.; Trabolsi, A.; Fang, L.; Olson, M. A.; Dey, S. K.; Grzybowski, B. A.; Stoddart, J. F. Molecular-Mechanical Switching at the Nanoparticle−Solvent Interface: Practice and Theory. *J. Am. Chem. Soc.* **2010**, *132*, 4310–4320.

(12) Huang, T. J.; Tseng, H.-R.; Sha, L.; Lu, W.; Brough, B.; Flood, A. H.; Yu, B.-D.; Celestre, P. C.; Chang, J. P.; Stoddart, J. F. Mechanical Shuttling of Linear Motor-Molecules in Condensed Phases on Solid Substrates. *Nano Lett.* **2004**, *4*, 2065–2071.

(13) Nørgaard, K.; Laursen, B. W.; Nygaard, S.; Kjaer, K.; Tseng, H.-R.; Flood, A. H.; Stoddart, J. F.; Bjørnholm, T. Structural Evidence of Mechanical Shuttling in Condensed Monolayers of Bistable Rotaxane Molecules. *Angew. Chem., Int. Ed.* **2005**, *44*, 7035–7039.

(14) DeIonno, E.; Tseng, H.-R.; Harvey, D. D.; Stoddart, J. F.; Heath, J. R. Infrared Spectroscopic Characterization of [2]Rotaxane Molecular Switch Tunnel Junction Devices. *J. Phys. Chem. B* **2006**, *110*, 7609–7612.

(15) Collier, C. P.; Mattersteig, G.; Wong, E. W.; Luo, Y.; Beverly, K.; Sampaio, J.; Raymo, F. M.; Stoddart, J. F.; Heath, J. R. A [2]Catenane-Based Solid State Electronically Reconfigurable Switch. *Science* **2000**, *289*, 1172–1175.

(16) Luo, Y.; Collier, C. P.; Jeppesen, J. O.; Nielsen, K. A.; DeIonno, E.; Ho, G.; Perkins, J.; Tseng, H.-R.; Yamamoto, T.; Stoddart, J. F.

Two-Dimensional Molecular Electronics Circuits. *ChemPhysChem* **2002**, *3*, 519–525.

(17) Diehl, M. R.; Steuerman, D. W.; Tseng, H.-R.; Vignon, S. A.; Star, A.; Celestre, P. C.; Stoddart, J. F.; Heath, J. R. Single-Walled Carbon Nanotube Based Molecular Switch Tunnel Junctions. *ChemPhysChem* **2003**, *4*, 1335–1339.

(18) Green, J. E.; Choi, J. W.; Boukai, A.; Bunimovich, Y.; Johnston-Halperin, E.; DeIonno, E.; Luo, Y.; Sheriff, B. A.; Xu, K.; Shik Shin, Y. A 160-Kilobit Molecular Electronic Memory Patterned at 1011 Bits Per Square Centimetre. *Nature* **2007**, *445*, 414–417.

(19) Zhang, W.; DeIonno, E.; Dichtel, W. R.; Fang, L.; Trabolsi, A.; Olsen, J.-C.; Benítez, D.; Heath, J. R.; Stoddart, J. F. A Solid-State Switch Containing an Electrochemically Switchable Bistable Poly[*n*]rotaxane. *J. Mater. Chem.* **2011**, *21*, 1487–1495.

(20) Jang, S. S.; Jang, Y. H.; Kim, Y.-H.; Goddard, W. A.; Flood, A. H.; Laursen, B. W.; Tseng, H.-R.; Stoddart, J. F.; Jeppesen, J. O.; Choi, J. W. Structures and Properties of Self-Assembled Monolayers of Bistable [2]Rotaxanes on Au (111) Surfaces from Molecular Dynamics Simulations Validated with Experiment. *J. Am. Chem. Soc.* **2005**, *127*, 1563–1575.

(21) Jang, S. S.; Jang, Y. H.; Kim, Y.-H.; Goddard, W. A.; Choi, J. W.; Heath, J. R.; Laursen, B. W.; Flood, A. H.; Stoddart, J. F.; Nørgaard, K. Molecular Dynamics Simulation of Amphiphilic Bistable [2]Rotaxane Langmuir Monolayers at the Air/Water Interface. *J. Am. Chem. Soc.* **2005**, *127*, 14804–14816.

(22) McFarland, A. D.; Young, M. A.; Dieringer, J. A.; Van Duyne, R. P. Wavelength-Scanned Surface-Enhanced Raman Excitation Spectroscopy. *J. Phys. Chem. B* **2005**, *109*, 11279–11285.

(23) Witlicki, E. H.; Hansen, S. W.; Christensen, M.; Hansen, T. S.; Nygaard, S. D.; Jeppesen, J. O.; Wong, E. W.; Jensen, L.; Flood, A. H. Determination of Binding Strengths of a Host−Guest Complex Using Resonance Raman Scattering. *J. Phys. Chem. A* **2009**, *113*, 9450–9457.

(24) Berlinsky, A. J.; Hoyano, Y.; Weiler, L. Raman Spectra of Tetrathiafulvalene (TTF). *Chem. Phys. Lett.* **1977**, *45*, 419–421.

(25) Van Duyne, R. P.; Haushalter, J. P. Resonance Raman Spectroelectrochemistry of Semiconductor Electrodes: the Photooxidation of Tetrathiafulvalene at *n*-Gallium Arsenide(100) in Acetonitrile. *J. Phys. Chem.* **1984**, *88*, 2446–2451.

(26) Drozdova, O.; Yamochi, H.; Yakushi, K.; Uruichi, M.; Horiuchi, S.; Saito, G. Determination of the Charge on BEDO-TTF in its Complexes by Raman Spectroscopy. *J. Am. Chem. Soc.* **2000**, *122*, 4436–4442.

(27) Van Duyne, R. P.; Cape, T. W.; Suchanski, M. R.; Siedle, A. R. Determination of the Extent of Charge Transfer in Partially Oxidized Derivatives of Tetrathiafulvalene and Tetracyanoquinodimethan by Resonance Raman Spectroscopy. *J. Phys. Chem.* **1986**, *90*, 739–743.

(28) Van Duyne, R., P. Applications of Raman Spectroscopy in Electrochemistry. *J. Phys. Colloq.* **1977**, *38*, 239–252.

(29) Sandroff, C. J.; Weitz, D. A.; Chung, J. C.; Herschbach, D. R. Charge Transfer from Tetrathiafulvalene to Silver and Gold Surfaces Studied by Surface-Enhanced Raman Scattering. *J. Phys. Chem.* **1983**, *87*, 2127–2133.

(30) Nie, S.; Yu, N.-T. Surface-Enhanced Near-Infrared Fourier Transform Raman Scattering of Tetrathiafulvalene Adsorbed on Silver Powder. *J. Raman Spectrosc.* **1991**, *22*, 489–495.

(31) Joy, V. T.; Srinivasan, T. K. K. SERS Studies on Tetrathiafulvalene, Diphenyltetrathiafulene and Octahydrodibenzotetrathiafulvalene. *Chem. Phys. Lett.* **2000**, *328*, 221–226.

(32) Cooke, G.; Duclairoir, F. M. A.; Rotello, V. M.; Stoddart, J. F. The Reversible Complexation of a Tetrathiafulavene Functionalised Self-Assembled Monolayer by Cyclobis(paraquat-*p*-phenylene). *Tetrahedron Lett.* **2000**, *41*, 8163–8166.

(33) Bryce, M. R.; Cooke, G.; Duclairoir, F. M. A.; John, P.; Perepichka, D. F.; Polwart, N.; Rotello, V. M.; Stoddart, J. F.; Tseng, H.-R. Surface Confined Pseudorotaxanes with Electrochemically Controllable Complexation Properties. *J. Mater. Chem.* **2003**, *13*, 2111–2117.

(34) Yokota, Y.; Miyazaki, A.; Fukui, K.-I.; Enoki, T.; Tamada, K.; Hara, M. Dynamic and Collective Electrochemical Responses of Tetrathiafulvalene Derivative Self-Assembled Monolayers. *J. Phys. Chem. B* **2006**, *110*, 20401–20408.

(35) Hulteen, J. C.; Van Duyne, R. P. Nanosphere Lithography: A Materials General Fabrication Process for Periodic Particle Array Surfaces. *J. Vac. Sci. Technol., A* **1995**, *13*, 1553–1558.

(36) Willets, K. A.; Van Duyne, R. P. Localized Surface Plasmon Resonance Spectroscopy and Sensing. *Annu. Rev. Phys. Chem.* **2007**, *58*, 267–297.

(37) Bard, A. J. F., L. R., *Electrochemical Methods: Fundamentals and Applications*, 2nd ed.; John Wiley and Sons, Inc: Hoboken, NJ, 2001.

(38) Love, J. C.; Estroff, L. A.; Kriebel, J. K.; Nuzzo, R. G.; Whitesides, G. M. Self-Assembled Monolayers of Thiolates on Metals as a Form of Nanotechnology. *Chem. Rev.* **2005**, *105*, 1103–1170.

(39) Wang, Y.; Kaifer, A. E. Interfacial Molecular Recognition. Binding of Ferrocenecarboxylate to β-Aminocyclodextrin Hosts Electrostatically Immobilized on a Thioctic Acid Monolayer. *J. Phys. Chem. B* **1998**, *102*, 9922–9927.

(40) Wan, L.-J.; Terashima, M.; Noda, H.; Osawa, M. Molecular Orientation and Ordered Structure of Benzenethiol Adsorbed on Gold(111). *J. Phys. Chem. B* **2000**, *104*, 3563–3569.

(41) Dong, Y.; Abaci, S.; Shannon, C.; Bozack, M. J. Self-Assembly and Electrochemical Desorption of Thioctic Acid Monolayers on Gold Surfaces. *Langmuir* **2003**, *19*, 8922–8926.

(42) Frisch, M. J.; Trucks, G. W.; Schlegel, H. B.; Scuseria, G. E.; Robb, M. A.; Cheeseman, J. R.; Zakrzewski, V. G.; J. A. Montgomery, J.; Stratmann, R. E.; J. C. Burant, S. D., *GAUSSIAN98*, revision A.11.2; Gaussian, Inc.: Pittsburgh, PA, 1998.

(43) Moskovits, M. Surface Selection Rules. *J. Chem. Phys.* **1982**, *77*, 4408–4416.

(44) Laviron, E. The Use of Linear Potential Sweep Voltammetry and of A.C. Voltammetry for the Study of the Surface Electrochemical Reaction of Strongly Adsorbed Systems and of Redox Modified Electrodes. *J. Electroanal. Chem. Interfacial Electrochem.* **1979**, *100*, 263–270.

(45) Matsuda, H.; Aoki, K.; Tokuda, K. Theory of Electrode Reactions of Redox Couples Confined to Electrode Surfaces at Monolayer Levels: Part I. Expression of the Current-Potential Relationship for Simple Redox Reactions. *J. Electroanal. Chem. Interfacial Electrochem.* **1987**, *217*, 1–13.

(46) Matsuda, H.; Aoki, K.; Tokuda, K. Theory of Electrode Reactions of Redox Couples Confined to Electrode Surfaces at Monolayer Levels: Part II. Cyclic Voltammetry and AC Impedance Measurements. *J. Electroanal. Chem. Interfacial Electrochem.* **1987**, *217*, 15–32.